Ion flux composition in HBr/Cl2/O2 and HBr/Cl2/O2/CF4 chemistries during silicon etching in industrial high density plasmas

G. Cunge, R.L. Inglebert, O. Joubert, L. Vallier, N. Sadeghi

Ion flux composition in $HBr/Cl_2/O_2$ and $HBr/Cl_2/O_2/CF_4$ chemistries during silicon etching in industrial high-density plasmas

G. Cunge,[a] R. L. Inglebert, O. Joubert, and L. Vallier
Laboratoire des Technologies de la Microélectronique CNRS, CEA–LETI, 17 rue des Martyrs, 38054 Grenoble Cedex, France

N. Sadeghi
Laboratoire de Spectrométrie Physique, Université Joseph Fourier Grenoble-1, BP87, 38402 Saint Martin d'Hères, France

(Received 24 January 2002; accepted 12 August 2002)

Anisotropic etching of silicon gates is a key step in today's integrated circuit fabrication. For sub-100 nm gate dimensions, one of the main issues is to precisely control the shape of the etched feature. This requires a detailed knowledge of the various physicochemical mechanisms involved in anisotropic plasma etching. Since silicon etching in high-density plasmas is strongly ion assisted, the identities of the ions bombarding the wafer is a key parameter that governs the etch rates and the etched profiles. In the present article, mass spectrometry has been used to investigate the chemical composition of the ion flux bombarding the reactor walls of an industrial inductively coupled plasma used for 200-mm-diam silicon wafer processing. The plasma chemistries investigated are $HBr/Cl_2/O_2$ and $HBr/Cl_2/O_2/CF_4$ mixtures optimized for sub-100 nm gate processes. Quantitative ion mass spectra show that under those conditions the ion flux contains up to 50% of $SiCl_XBr_Y^+$ $(X,Y=0-2)$ ions, although Cl^+, Cl_2^+, and Br^+ ions were expected to be the predominant species. This observation can be explained by the combination of two well-accepted phenomena that are discussed in detail. The impact of the surprisingly large amount of ionized silicon-based etch products on silicon etching mechanisms are discussed. [DOI: 10.1116/1.1511219]

I. INTRODUCTION

Plasma etching[1] has been successfully used in the past 20 years for fine-pattern transfer in the active parts of ultra-large-scale integrated (ULSI) circuits. However, as the semiconductor industry continues to scale down the dimensions of ULSI circuits below 0.1 μm, more and more precise control of the line-shape profile of the etched features is required. In silicon gate etching the process must be highly anisotropic to control the critical dimension of the etched gates, *and* be defect free (e.g., without microtrenching) to keep a high selectivity towards the ultrathin oxide underlayer.

Such precise control of the shape of the features being etched requires detailed knowledge of the various etching (or deposition) mechanisms involved in a specific process. In order to optimize plasma etching processes with large processing windows, it is important to understand the basic etching mechanisms that control the etch anisotropy. At the same time, predictive etching profile evolution models must be developed for process control and development.[2] Several researchers have built simulation codes that predict the time evolution of a feature being etched in a specific chemistry by transporting ions and neutrals from the plasma to the surface.[3–11] However, if such simulation tools may help for faster development of specific etch processes, they rely on the understanding of the main physicochemical mechanisms occurring on a surface (with topography) exposed to reactive plasmas. The time evolution of the etched profile depends on many parameters, which are often unknown. For silicon etching these parameters include ion and neutral chemical nature and energy, fluxes, surface reaction probabilities, scattering probabilities, and angular distribution, together with the feature's sidewall chemical composition and other parameters such as the mask material and shape. Some of those quantities have been measured experimentally in recent high-density etching tools allowing validation and improvement of existing models. Sophisticated optical diagnostics[12] and mass spectrometry[13] have been used to investigate the chemical composition of the neutral species generated in the plasma gas phase, allowing, for example, the dissociation degree of the plasma to be measured.[14] Complementary information can be obtained from electrical (Langmuir probe) diagnostics, which provide a measurement of the ion fluxes bombarding the wafer,[15] and electron energy distribution function[16] that may be used to simulate the plasma gas phase chemical kinetics. Furthermore, surface studies using x-ray photoelectron spectroscopy (XPS) and spectroscopic ellipsometry have provided the chemical composition and thickness of the reactive layers driving the etching processes on the silicon surface, together with the chemical composition of the passivation layers deposited on the feature sidewalls.[17,18] Several important parameters of the plasma/surface interaction have not been measured yet (or cannot be measured experimentally), in particular, in industrial silicon etching tools. Modeling, therefore, relies on some assump-

[a]Electronic mail: CungeGi@chartreuse.cea.fr

tions of the values of some parameters, values often inspired from detailed molecular dynamics simulations,[19] which can provide scattering probabilities, for example. Other information required to simulate an etching process (such as etching yields and etched products distribution) are also directly extracted from ion beam experiments in which an energetic ion beam (usually Ar^+ or[20] Cl_X^+) bombards a silicon wafer, in the presence of a reactive neutral background gas (Cl_2, Cl, F). Winter and Coburn[21] have reviewed much of these experiments relevant to plasma-assisted etching. In such experiments the plasma surface interaction is, therefore, simulated by an "ideal" system in which the incident ions either provide kinetic energy to the surface (Ar^+ ions) or promote etching reactions through their chemical nature (Br^+, Cl_X^+, and F^+ ions). Most of the etching profile simulators used nowadays rely on the assumption that the incident ions bombarding the wafer consist solely of reactive species produced by direct ionization of the feed gas stock molecules (e.g., Cl^+, Cl_2^+, Br^+, HBr^+, F^+,...). However, chemistries used for silicon gate etching involve the mixture of several gases ($HBr/Cl_2/O_2/CF_4$), which may generate a large number of ionic species. Furthermore industrial high-density etching tools are processing large-diameter silicon wafers (200–300 mm diam) at fast etch rates (200 nm min^{-1}) and constant gas flow. As a result, in addition to processing gases introduced in the plasma chamber, a significant fraction of silicon etching by-products is present in the gas phase. These silicon-based species can be further dissociated and ionized in the plasma bulk resulting in significant density of halogenated silicon-containing ions in the total ion flux bombarding the wafer. Since silicon etching proceeds through the synergetic interaction of reactive neutral species and ions, the identity of the ions bombarding the wafer is a key parameter that will largely drive the etch process.

In the present article, quantitative mass spectrometry is used to investigate the chemical nature of the ion flux bombarding the reactor walls of an industrial silicon etcher operated in a standard $HBr/Cl_2/O_2$ chemistry. We will demonstrate that the ion flux chemical composition significantly differs from the expectations since it contains very large amounts of ionized $SiCl_XBr_Y^+$ species even for very short gas residence times. The influence of the plasma operating conditions (source power, bias power, initial chemistry) of the ion flux composition and the consequences expected on the etch process will be discussed.

II. EXPERIMENTAL SETUP AND APPARATUS

Etching experiments have been carried out on 200-mm-diam wafers in an industrial cluster tool, which consists of a load-lock chamber located in a class 10 clean room, a high-density decoupled plasma source [(DPS), Centura 5200 by Applied Materials, Inc.] and an XPS analysis chamber, all three connected together via a robotized transfer chamber. The inductive source consists of a ceramic dome around which is wrapped a three-dimensional coil. Radio-frequency power at 12.56 MHz is supplied to the antennas through an automatic matching network in a power range between 200 and 1200 W (Fig. 1). The 200 mm wafers can be biased independently with a 0–200 W rf power supply operated at 13.56 MHz. The lower electrode has a monopolar electrostatic chuck (ESC) with polyimide coating. The wafer temperature is kept at 50 °C by helium backside cooling, while the walls of the chamber are kept at 70 °C by separate heat exchangers. The ceramic dome is air cooled when the plasma is on and is heated by infrared lamps when the chamber is idle, providing a constant temperature of 60 °C. The etch gases used in this study are Cl_2, HBr, O_2, and CF_4. Gases are introduced into the chamber through four symmetric nozzles on the chamber walls (at the same position as the mass spectrometer in Fig. 1) and are pumped by a 2000 l s^{-1} turbomolecular pump. This gas injection configuration may influence the neutral transport, and in particular the etch product recycling, as discussed by Kiehlbauch and Graves.[22] In all the experiments, the total gas flow rate is about 200 sccm and the pressure is kept constant at 4 mTorr by adjusting the pumping rate with an automatic throttle valve between the chamber and the turbopump. These experimental conditions correspond to a residence time of about 55 ms (the reactor volume is 35 l). Experiments are carried out while etching blanket silicon wafers in a $HBr/Cl_2/O_2$ gas mixture.

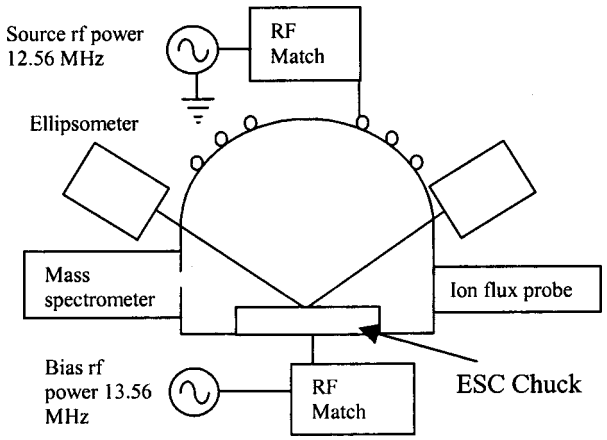

FIG. 1. Schematics of the experimental setup.

Additional ports have been added to the DPS chamber with respect to its standard configuration so that the chamber can host several *in situ* diagnostics, including a kinetic ellipsometer for etch rate measurements, a mass spectrometer, and an ion flux probe (Fig. 1). A Scientific System, Inc. ion flux probe[23] is used to calibrate the mass spectrometer in all the different experiments. This probe is located at the reactor walls in a position symmetric to the entrance hole of the mass spectrometer with respect to the center of the plasma chamber, and provides the value of the total ion flux bombarding the reactor walls.

Mass spectrometric experiments are performed using a Hiden Analytical EQP analyzer connected to the plasma-etch chamber walls (Fig. 1). The probe of the mass spectrometer is composed of five sections: the extractor, the RGA source, energy analyzer, quadrupole mass filter, and detector. The probe is differentially pumped by a turbomolecular pump (60

$1\,s^{-1}$), which allows a base pressure of $10^{-6}-10^{-7}$ Torr to be reached in the mass spectrometer (depending on the processing pressure in the plasma chamber). By biasing the extractor, analyses of either ions or neutrals extracted from the plasma is, in principle, possible. However, because neutral detection by mass spectrometry requires careful attention and specific differentially pumped systems,[24,25] we have only used the mass spectrometer in the ion analysis mode. In this mode, the positive ion Bohm flux leaving the plasma is sampled through a 50-μm-diam sampling orifice (located at the reactor wall), behind which the extractor is placed. The ions are then focused in the ion transport system, energy selected, and detected. In this operating mode, the ion energy distribution function (IEDF) at a given mass is first measured in order to choose the optimum pass energy. This energy, which corresponds to the IEDF's maximum intensity, is then chosen as the pass energy for all the ions present in the plasma. This approach is valid only if the IEDF of all ions are single peaked (around the dc value of the plasma potential).[26] The validity of this assumption is checked under our conditions by comparing several mass spectra measured at different passing energy.[26] The result shows an excellent reproducibility between the mass spectra for masses above 30 amu. As a result, the pass energy is always chosen at the maximum of the IEDF of Br^+ ions (79 amu) and kept constant during the mass spectrum acquisition. Using this technique, we estimate that the signal at masses below 30 amu is slightly underestimated (10%–30%) compared to higher mass peaks.

Furthermore, the mass spectrometer transmission as a function of the mass has been calibrated using two different techniques. In the first one,[27] we used rare gas plasmas (either argon, krypton, or xenon), where only one specific ion (and its isotopes) dominates the mass spectrum (e.g., Ar^+ at 40 amu, Kr^+ at 84 amu, or Xe^+ at 132 amu). For each of these three plasmas, the ion flux probe is used simultaneously to tune the rf source power to keep constant the ion flux entering the mass spectrometer. The ion flux being constant in each case and consisting only of a single species ions, sensitivity S of the mass spectrometer at mass $m=84$ and 132 (relative to that at 40 amu) is simply given by $S^m=[I^m*(100/\alpha)/I^{m=40}]$, where I^m is the peak signal (measured as the integral of the IEDF at mass m) and α is the percentage of the considered isotope of mass m. The validity of this calibration technique was checked by detecting neutral species (without plasma) in the RGA mode where the neutrals entering the mass spectrometer are ionized by 20, 50, and 70 eV electrons. At a constant gas pressure in the chamber (Ar, Kr, or Xe) and for a given electron energy, the signal I^m at each mass m must then be directly proportional to the ionizing cross section σ at the considered electron energy. The sensitivity of the mass spectrometer at $m=84$ and 132 relative to $m=40$ is then given by[13] $S^m=[\sigma^{Ar}*I^m*(100/\alpha)]/[\sigma^m*I^{Ar}]$. These two calibration techniques agree within 25% (this deviation between the two techniques is attributed to uncertainties in the value of the ionizing cross section), leading to $S^{84}=0.4$ and $S^{132}=0.19$ (taking $S^{Ar}=1$). The sensitivity at any mass is then assumed to be $S=1$ for $m<40$ amu, and to decay for $m>40$ according to $S_{m>40}=0.089+2.42*\exp(-m/40{,}96)$.

In the following, all the mass spectra presented are first corrected by the mass sensitivity $S(m)$ of the spectrometer, and then calibrated on an absolute scale by equating the total ion flux bombarding the walls (measured by the ion flux probe) with the sum of all the mass peaks present in the mass spectra. Using this method, mass spectra are converted from counts s^{-1} to mA cm^{-2}, and mass spectra measured during different plasma conditions can be directly compared between each other on an absolute scale. The total uncertainty in the calibrated mass spectra is estimated to be around 40% when comparing low and high mass peaks.

Each experiment is performed after cleaning the reactor walls using a $SF_6/Cl_2/O_2$ plasma and then conditioning the walls again by running the processing plasma to be analyzed for 1 min. Furthermore, a new blanket silicon wafer is used for each measurement, allowing a good reproducibility of the results obtained.

III. RESULT AND DISCUSSION

A. Chemical composition of the ion flux during a gate etch process

Sub-100 nm silicon gate etching is performed in high-density inductively coupled plasmas (ICPs) operated in a so-called ''standard'' chemistry, which consists of a mixture of HBr/Cl_2 and O_2 gases. The addition of O_2 to the HBr/Cl_2 mixture results in the formation of a silicon oxychloride ($SiO_XCl_YBr_Z$) passivation layer on the sidewall of the photoresist[17] and on the sidewalls of the silicon features.[8,18] To begin this study, an etching process is first optimized according to 0.1 μm integrated circuit (IC) generation requirements. The optimized process conditions are 4 mTorr total pressure in a HBr (110 sccm)/Cl_2 (70 sccm)/O_2 (5 sccm) gas mixture with 450 W rf source power and 100 W rf bias power. The etching profile of a 70 nm isolated line etched through a 40-nm-thick oxide hard mask with this process is shown in Fig. 2, demonstrating an excellent profile control in terms of anisotropy and absence of structural defects in the 2 nm gate oxide.

The ion mass spectrum recorded on blanket wafers under these conditions is shown in Fig. 3 while the chemical composition of the ion flux is summarized in Table I. Figure 3 shows that many reactive species are found in the composition of the ion flux, demonstrating the complexity of an industrial etching process. Indeed, contrary to the well-accepted models assuming that the incoming ion flux consists mainly of reactive ions such as Cl^+ and Br^+, Table I indicates that under the processing conditions studied here, these halogen ions represent less than 50% of the total ion flux. On the other hand, the ions bombarding the reactor walls (and, therefore, the wafer) include large amounts of $SiCl^+$ and significant densities of $SiCl_3^+$, Si^+, $SiCl_2^+$, $SiBr^+$, and $SiCl_2Br^+$ ionized etch products. Similar mass spectra are also observed on patterned wafers, since large

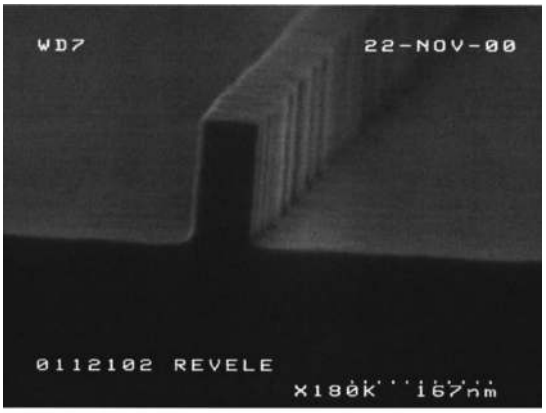

FIG. 2. Etch profile of a 70 nm silicon line etched through a 40-nm-thick SiO_2 hard mask. The main etching step process conditions are 4 mTorr total pressure in an HBr (110 sccm)/Cl_2 (70 sccm)/O_2 (5 sccm) gas mixture with a 450 W rf source power and 100 W rf bias power. The silicon film thickness is 150 nm and the underlying gate oxide thickness is 2 nm.

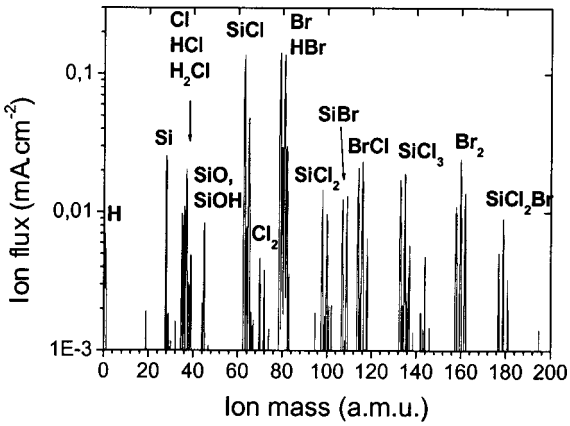

FIG. 3. Calibrated ion mass spectrum of a 4 mTorr total pressure in a HBr (110 sccm)/Cl_2 (70 sccm)/O_2 (5 sccm) gas mixture with a 450 W rf source power and 100 W rf bias power.

open areas (typically 50%) are layed out on the silicon wafer at the gate level.

The experimental result shown in Fig. 3 contradicts many widespread ideas about etching in halogen-based chemistries and has severe consequences on modeling studies (since these measurements are performed in a real industrial plasma using a typical etching recipe for sub-100 nm gates generation). Similar observations have been reported by Goyette *et al.*[28,29] in fluorocarbon plasmas operated without a wafer in a Gaseous Electronics Conference (GEC) reactor cell. They reported that the dominant ions are not originating from direct ionization of the feed gas stock molecules, and that Si^+ ion dominates the mass spectra in CHF_3 plasmas.

As discussed below, under our low-pressure conditions, the mean-free path for charge transfer from an HBr^+ ion to a $SiCl_X$ neutral etch product is large, and it is, therefore, expected that the chemical composition of the ion flux is roughly similar at the reactor walls and at the wafer. Therefore, Fig. 3 indicates that large fluxes of silicon-containing products are bombarding the silicon wafer during real processes. Indeed, even with large gas flow rates significant concentrations of $SiCl_XBr_Y$ silicon-based etch products are present in the gas phase during etching of large size wafers at a high rate. Under our conditions, at a pressure of 4 mTorr, a total gas flow rate of about 200 sccm corresponds to an incoming flux of "reactive species" of around 9×10^{19} molecules s^{-1}. At the same time, the etch rate is around 200 nm min^{-1}, which corresponds to an out coming equivalent silicon flux of 5.2×10^{18} atoms s^{-1} (for a blanket 200-mm-diam silicon wafer). Therefore, in a steady-state processing regime, the flow of silicon-containing species produced by the wafer represents approximately 6% of the halogen parent gas flow injected into the reactor.

Furthermore, the concentration of reactive halogen atoms such as Cl in the gas phase is determined by the difference between its production rate (electron impact dissociation of Cl_2, HCl, and $SiCl_X$ in the plasma volume) and its loss rate on the reactor walls, at the wafer surface and by chemical reactions in the gas phase. At low pressures, where diffusion transport to the walls is fast (and volume losses are negligible), the surface loss of neutral species (etching or recombination reactions) will strongly influence their average concentrations in the plasma volume. As a result, high etch rates of silicon will consume Cl and Br atoms at a large rate, thereby decreasing their gas phase concentrations (loading effect). Therefore, the ratio of halogenated silicon neutrals to halogen molecules depends on the etch rate, on the Cl_2 and HBr gas flows, on the dissociation rate, and the surface loss probability of these species at the wafer surface and reactor walls. The loading mechanism by the wafer is illustrated in Fig. 4, where we show the ion mass spectrum measured under the same condition as in Fig. 3 but without bias power. Under those conditions, the etch rate is greatly reduced (the substrate is floating and therefore bombarded only by 15–20 eV ions) and the loss rate of halogen neutrals at the silicon surface significantly drops. As a result, Br^+ ions become the predominant species of the ion flux.

However, loading effects cannot explain the high ratio of silicon-containing ion density relative to the halogen ion density measured in Fig. 3. The density ratio SiX^+/X^+ (where X is a halogen) of silicon-containing ions to halogen ions is not directly related to the parent neutral concentration ratio [SiX]/[X]. If dissociative ionization and charge exchange are neglected, the density of a given ion X^+ in the plasma is not only proportional to the partial pressure of its parent neutral [X] but depends on the neutral partial pressure [X] and the ionization rate, which in first approximation (Maxwellian EEDF with temperature T_e) can be written as

$$[X^+]\propto[X]\langle\sigma v\rangle\exp(-E_i/T_e), \tag{1}$$

where $\langle\sigma v\rangle$ is the average value of the product of the electron impact cross section by the electron mean speed and E_i is the energy threshold for ionization assumed to be at least several times T_e. Although the cross sections for $SiCl_XBr_Y$ etch products are unknown, the ionization threshold in energy of etch products can be found in the literature. For example, the ionization energies of Cl^{35} and Br^{79} are 12.97

TABLE I. Chemical composition of the ion flux bombarding the reactor walls in the 4 mTorr, HBr (110 sccm)/Cl_2 (70 sccm)/O_2 (5 sccm) gas mixture, with 450 W rf source power and 100 W rf bias power. The numbers include the sum over all the isotopes of Cl and Br.

Species	Br	SiCl	HBr	BrCl	Br_2	$SiCl_3$	H_XCl	Si^+ SiH	$SiCl_2$	SiBr	Cl	SiO^+ SiOH
% of total ion flux	32.7	22.9	7.3	6.3	5.5	5.1	4.1	3.3	3.3	3.1	1.5	1.2

and 11.81 eV, respectively, whereas the ionization energies of Si, SiBr, SiF, and SiCl are 7.41, 7.3, 7.28, and 6.79 eV, respectively. Now, let us consider a pure 4 mTorr Cl_2 plasma being 100% dissociated. Without considering loading effects, this leads to an upper limit for [Cl] atom concentration in the gas phase of about 1.3×10^{14} cm^{-3}, while typical etching by-product concentrations are expected to lie around 5×10^{12} cm^{-3} (as measured by broadband UV absorption spectroscopy in Cl_2 ICP plasmas at similar etch rates[30]). In a rough approximation we can consider that the ratio [Cl]/[SiCl] is around 25 in the gas phase of a low-pressure high-density plasma. Assuming a 3 eV electron temperature, the exponential terms in Eq. (1) imply that the corresponding ionic ratio $[Cl^+]/[SiCl^+]$ is only about 3.3 (both the differences in σ and the contribution from dissociative ionization are neglected here). The fact that the charge in the plasma will preferentially be transferred to the lowest ionization potential species by electron impact was observed in the simulation of Lee, Graves, and Lieberman[31] and has been mentioned in a recent paper of Vitale, Chae, and Sawin.[32] Therefore, the large density of silicon-containing ions relative to halogen ions that we measure in the ion flux bombarding the reactor walls can be explained first by loading effects decreasing the neutral halogen atoms concentrations, and second by a lower ionization energy threshold of halogenated silicon etch by products relative to halogen atoms.

As an alternative explanation, charge exchange reactions may also be considered to explain such a large density of silicon-containing ions: $SiCl_X + X^+ \rightarrow SiCl_X^+ + X$, where X^+ is the predominant halogen ion in the plasma. This reaction will be, in principle, favorable due to the lower ionization energy of the etch products when compared to halogen atoms. However, this type of reaction will be important for the ion chemistry only if it produces $SiCl_X^+$ ions at a faster rate than the direct ionization, e.g., $SiCl_X + e^- \rightarrow SiCl_X^+ + 2e^-$. Figure 5 shows the reaction rates for these different processes as a function of electron temperature. The reaction rates for the electron impact ionization of Si and SiCl were taken from Lee, Graves, and Lieberman.[31] The reaction rates for charge exchange reactions (dotted lines in Fig. 5) are an upper limit because we are assuming a very large cross section (10^{-14} cm^{-2}) for all asymmetric charge exchange reactions, and a mean thermal velocity of 5×10^4 $cm\,s^{-1}$. If we further consider that, as in a Cl_2 discharge[33] at 4 mTorr, the total density of X^+ ions is of the same order of magnitude as the electron density, and that the electron temperature lies in between 3 and 3.5 eV, then Fig. 5 demonstrates that at 4 mTorr the production rates of Si^+ and $SiCl^+$ ions (e.g., the predominant ions observed in these experiments) are largely dominated by electron impact ionization. However, we would like to underline that at higher pressures, where the electron temperature is lower, the charge exchange reaction may also influence the ion chemistry. Finally, charge exchange reactions in between etch products (such as $Si^+ + SiCl_4 \rightarrow SiCl^+ + SiCl_3$) may have a cross section as large as 150 A^2 at thermal energy,[34] but they will proceed at a very low rate due to the low densities of Si^+ ions and of $SiCl_4$ neutral etch products. As a conclusion, under our experimental conditions, charge exchange reactions between etch product ions and halogen atoms and molecules are not expected to play a significant role on the ion chemistry.

Finally, in addition to halogen ions and halogenated silicon ions resulting from ionization of the initial feedstock gas and etching products, the other species detected in significant

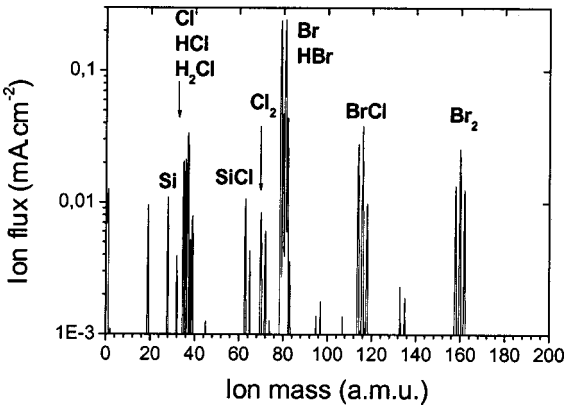

FIG. 4. Identical to Fig. 3 but without the bias power.

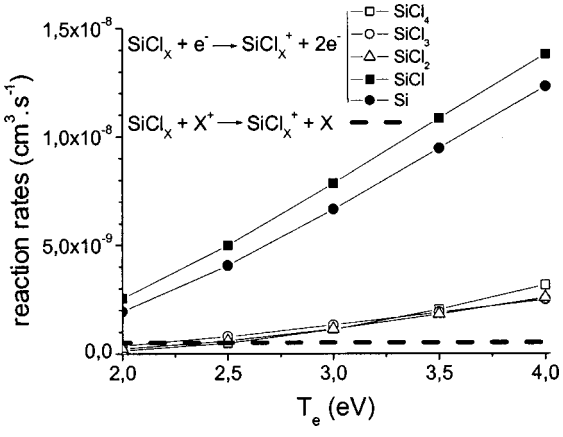

FIG. 5. Reaction rates (in $cm^3\,s^{-1}$) for electron impact ionization of the $SiCl_X$ etch product ($X=0-4$) as a function of the electron temperature. The dotted lines are upper values for the rate of nonresonant charge exchange reactions producing $SiCl_X^+$ ions, showing that they are small compared to direct ionization.

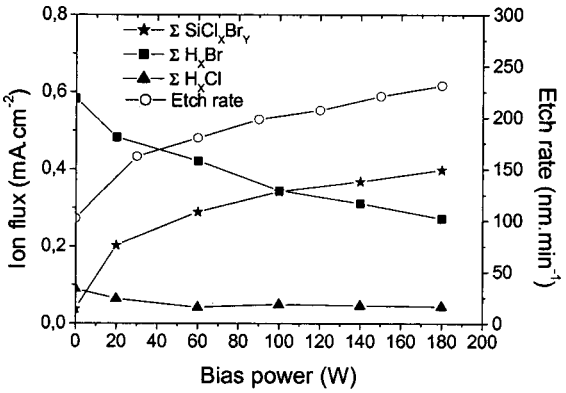

FIG. 6. Effect of the rf bias power (other process conditions as in Fig. 3) on the etch rate and on the density of halogenated silicon ions (sum of all of the $SiCl_XBr_Y$ with $0<X,Y<3$) and halogenated ions (sum of all $H_X{}^{79-81}Br$ and $H_X{}^{35-37}Cl$ ions with $X=0-2$).

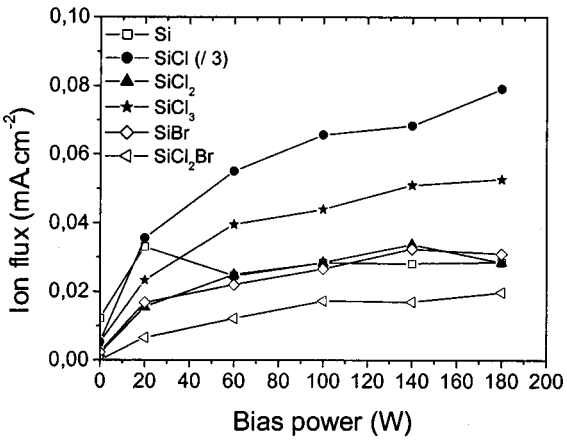

FIG. 7. Effect of the rf bias power on the density of several ionized etch products. Same processing conditions as in Fig. 6.

densities in Fig. 3 include $Br_2{}^+$ and $BrCl^+$ ions (resulting from recombination reactions of halogen atoms at the reactor walls and from chemical reactions in the gas lines), SiO^+ ions, and H^+ protons. We also note that proton attachment appears to be an important mechanism in this HBr-rich chemistry, since many of the detected ions are hydrogenated. This is illustrated by the higher intensity of mass 37 amu relative to mass 35, although the isotopic ratio of $^{35}Cl/^{37}Cl$ is supposed to be 1/0.32: the peak at $m=37$ is not only composed of ^{37}Cl but also contains a large amount of $H_2{}^{35}Cl^+$. Based on its orbital configuration, H_2Cl is an unstable molecule and direct electron impact ionization to produce H_2Cl^+ ion must be discarded. A plausible pathway for the production of this ion could be the direct proton attachment ($H^+ + HCl$). Based on the high polarizability of HCl molecules, this reaction is expected to have a very large cross section. As the concentration of neutral HCl molecules in the chamber is large, the production rate of H_2Cl^+ by proton attachment could be significant. In fact, HCl is already present in a large concentration in the initial gas mixture since mixing HBr and Cl_2 gases produces HCl molecules inside the gas line, as measured by the mass spectrometer working in the RGA mode, in the absence of plasma.

B. Effect of the plasma operating condition on the ion flux chemistry

1. Influence of bias power

The influence of the rf-bias power on the ion chemical distribution is summarized in Fig. 6. In this graph, we have reported the sum of the fluxes of all $SiCl_XBr_Y{}^+$ ($X,Y=0-2$) ions (largely dominated by $SiCl^+$ under these conditions), the total flux of H_XBr and H_XCl ions ($X=0-2$), and the etch rate obtained from ellipsometric measurements on Si-coated SiO_2 wafers. Figure 6 shows that increasing the ion energy deeply modifies the chemical composition of the ion flux. However, since the total ion flux collected by the ion flux probe (hence, the electron density) does not change by more than 5% between 0 and 180 W bias power, and since the charge exchange reaction may be neglected, we can conclude that the neutral concentration roughly follows the corresponding ion densities shown in Fig. 6. Indeed, the sum of the silicon-containing ion densities closely follows the etch rate, indicating that they originate from the ionization of silicon etch products.

As discussed previously, very large loading effects are also observed in Fig. 6: as the etch rate increases by a factor of 2, the Br^+ ion density drops by a factor of 2. As a result, for bias powers above 140 W, halogenated silicon ions represent more than 50% of the total ion flux impinging the wafer and reactor walls. The measured Cl^+ ion density is always very small, suggesting that Cl atoms are heavily loaded not only by the wafer but also by the reactor walls.

Figure 7 gives a more detailed picture of the different halogenated silicon ion behaviors as a function of the bias power. $SiCl^+$ appears to be the predominant ion under all conditions, followed by $SiCl_3{}^+$, while $SiCl_2{}^+$, $SiBr^+$, and Si^+ are present in similar densities. SiCl species can be formed in the gas phase following dissociation of $SiCl_2$ and $SiCl_4$ primary etch products, or can be produced directly at the wafer surface under high-energy ion bombardment conditions. Under our experimental conditions, where the energy of the ions reaching the wafer is above 100 eV, chemical sputtering is an important mechanism, producing elemental Si and SiCl as etch products.[35–38] All the $SiCl_XBr_Y$ ($X,Y \geqslant 1$) ion signals increase as the square root of the ion energy (proportional to the bias power at fixed total ion density), showing that they originate from the dissociation (and ionization) of etch by-products chemically sputtered in the gas phase during the etch process.

2. Influence of the source power on the ion flux composition

Figure 8 shows the variation of halogen and silicon-containing ions as a function of the source power, the total ion flux bombarding the reactor walls, and the etch rate. The experiment is carried out at a constant ion energy of roughly 200 eV (estimated from the rf-bias peak voltage V_{bias}) and not at constant bias power. In a first-order approximation,

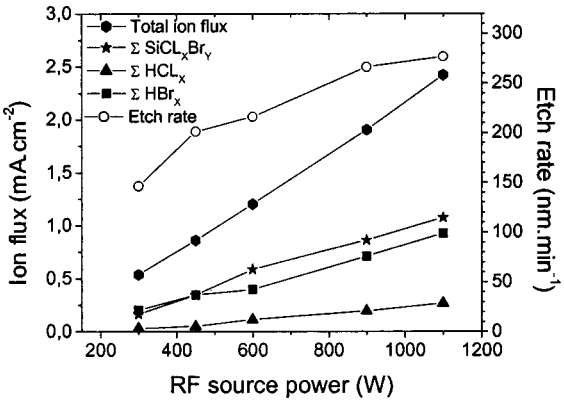

FIG. 8. Effect of the rf source power on the etch rate and on the density of halogenated silicon ions (sum of all of the $SiCl_XBr_Y$ with $0<X,Y<3$), halogenated ions (sum of all $H_X{}^{79-81}Br$ and $H_X{}^{35-37}Cl$ ions with $X=0-2$), and total ion flux. The pressure and gas mixture were identical to Fig. 3, and the rf bias power was adjusted so as to keep a constant ion energy.

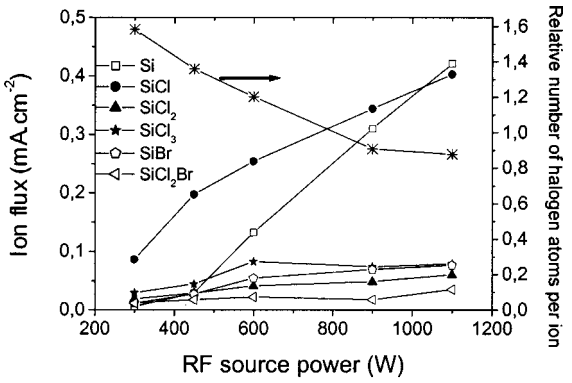

FIG. 9. Effect of the rf source power on the density of several ionized etch products and on the number of halogen atoms per incident halogenated ion showing that dissociation rate is increasing with rf power. Processing conditions identical to Fig. 8.

these two quantities are related by $P_{\text{bias}}=V_{\text{bias}}^{*}I$ where I is the total ion current to the wafer. Halogenated silicon ions represent about 30% of the total ion flux at a 300 W source power, and increase rapidly to 45%–50% for source powers higher than 600 W. This result is attributed to the combined effect of an increasing etch product concentration in the gas phase and a higher plasma density (the etch rate increases nonmonotically from 146 to 276 nm min^{-1} and levels off at the highest rf powers). Although not observed in Fig. 8, loading of halogen atoms by the silicon wafer is expected to increase when the etch rate increases. However, this effect is masked by an increasing dissociation rate of the feed gas stock molecules and etch products, finally generating a net increase in the Br and Cl atom concentrations (resulting in an increase of the ΣH_XBr^+ and ΣH_XCl^+ ion density). Furthermore, the situation is also complicated by possible changes in the electron energy distribution function (due to changes in neutral composition inside the chamber), which may change the cracking patterns of neutral species when the rf power is increased. Therefore, we are not able to fully explain the relationship between the etch rate and the ion flux in Fig. 8.

The chemical distribution of silicon-halogenated ions under these conditions is shown in Fig. 9. Also plotted in Fig. 9 is the average number N of halogen atoms per incident silicon-halogenated ions deduced from

$$N=\left(\left[\sum_{X,Y} X^{*}[SiCl_XBr_y{}^{+}]\right]+\left[\sum_{X,Y} Y^{*}[SiCl_XBr_y{}^{+}]\right]\right)\Big/\sum_{X,Y=0-2}[SiCl_XBr_Y{}^{+}]. \quad (2)$$

N is expected to be indicative of the halogenated silicon ion reactivity since $N<1$ means that after neutralization and fragmentation on the surface, these ions bring more silicon than halogen atoms to the surface while $N>1$ indicates a more reactive nature for these ions. Figure 9 shows that N starts at a value of 1.6 at low source power and decreases toward 0.9 at higher source power, which is a consequence of the increasing dissociation rate with rf power (and also possibly indicates that the etching becomes more physical as the ion flux increases). This is illustrated in Fig. 9, which shows that the density of Si^+ ions is increasing with rf power at a much faster rate than that of higher-order $SiCl_X$ ions, suggesting that the high degree of dissociation leads to the formation of elemental silicon in the gas phase. Indeed, for powers above 1 kW, Si^+ is becoming the principal ion. Such a large amount of Si^+ ions indicates that a significant density of silicon atoms are present in the plasma gas phase during processing at high power in agreement with the modeling results of Lee, Graves, and Lieberman.[31] These atoms (and ions) can stick on the chamber walls and wafer surfaces with a high probability. These Si atoms are, therefore, potential precursors for the passivation layer formation on the feature sidewalls[6,39] and reactor walls [by the mechanism: $Si(g)+O(g)+Si(s)\rightarrow SiO(s)$]. Broadband UV absorption experiments performed by Neuilly[30] also show a large absorption peak of atomic silicon at 288.1 nm, while the emission of atomic silicon at 288.1 nm is often used as an end point diagnostic in gate etch processes.

3. Influence of oxygen flow rate

The oxygen flow rate is a critical parameter regarding profile control since it drives the passivation layer formation (i.e., thickness) protecting the feature sidewalls.[40] The oxygen flow rate also influences the Si/SiO_2 and resist mask/Si etch selectivity.[41] Furthermore, the oxygen concentration has also an impact on the silicon etch rate: several authors[41,42] have reported that a small oxygen concentration (<10% of O_2 concentration) in halogen chemistries slightly enhances the silicon etch rate while a higher O_2 concentration results in a rapid decrease of the etch rate.

Figure 10 summarizes at standard conditions (4 mTorr, 450 W source rf power, and 100 W rf bias power) the effect of O_2 flow rate on the silicon etch rate, halogen ions, and halogenated silicon ion fluxes to the chamber walls. Figure 10 shows that the etch rate increases up to 10 sccm O_2 in the

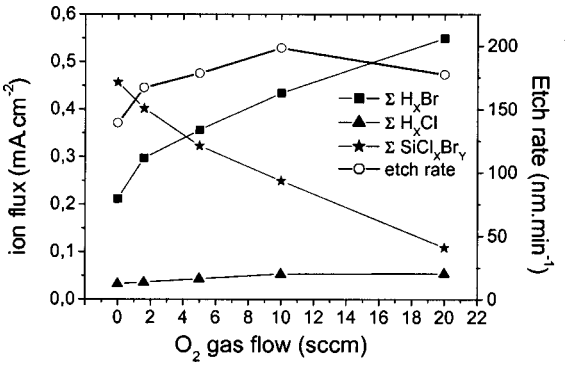

FIG. 10. Effect of the O_2 gas flow rate on the etch rate and on the density of halogenated silicon ions (sum of all of the $SiCl_XBr_Y$ with $0<X,Y<3$) and halogenated ions (sum of all $H_X{}^{79-81}Br$ and $H_X{}^{35-37}Cl$ ions with $X=0-2$). Other processing conditions identical to Fig. 3.

gas mixture and then slightly decreases. One consequence expected is that the sum of $SiCl_XBr_Y{}^+$ ions should increase with O_2 flow rates up to 10 sccm while at the same time loading effects must induce a decrease of Br and Cl densities. However, the opposite behavior is observed in Fig. 10: as O_2 flow rate increases from 0 to 20 sccm, the halogenated silicon ion density drops by roughly a factor of 5, while at the same time the bromine ion density increases by a factor of 2.5 (and Cl by 1.6). This apparent contradiction can be explained as follows:

The addition of O_2 to the gas mixture has a great impact on the chemical composition of reactive layers deposited on the reactor walls, which may in turn affect the species gas phase concentration by changing their surface loss probability. Such a loading effect by the chamber walls affects the halogen atom[43] density, and may influence[29] the gas phase concentration of $SiCl_X$ species. Under our conditions where the plasma species deposition induces a SiO_X-like layer on the walls, the wall reactivity with respect to $SiCl_XBr_Y$ and Cl (or Br) species is expected to be impacted by the atomic oxygen flux according to the following phenomenological reactions:

$$(SiCl_XBr_Y,\ SiCl_XBr_Y{}^+)_g+(O)_g+\text{surface}\rightarrow(SiO_zCl_w)_s, \tag{3}$$

$$(SiCl_XBr_Y)_s \quad \text{or} \quad (SiO_zCl_XBr_Y)_s+(Cl,Br)_g \rightarrow(SiCl_4,SiBr_4)_g, \tag{4}$$

$$(Cl,Br)_s+(Cl,Br)_g\rightarrow(Cl_2)_g,\ (Br_2)_g,\ (BrCl)_g, \tag{5}$$

where subscripts *s* and *g* represent the chamber wall surface and the gas phase, respectively. Equation (3) indicates that SiO_X layer formation proceeds through oxidation of silicon etch products adsorbed on the reactor walls. This surface reaction has been suggested[39] to be a plausible growth mechanism for SiO_X layers and it has been recently shown that it takes place during Cl_2/O_2 plasma etching of silicon.[44] Equation (4) accounts for SiO_X layer etching, and thus Cl and Br loading from the gas phase.

It is known that the chamber walls are kept "clean" without oxygen addition in the gas phase (no SiO_X deposition on the chamber walls). In this case the $SiCl_XBr_Y$ etch products sticking on the reactor walls are recycled[29] by forming $SiCl_4$ and $SiBr_4$ [Eq. (4)], leading to a strong loading of Br and Cl atom concentrations in the gas phase (which explains the large [SiX]/[X] ratio observed in Fig. 10 at zero O_2 concentration). By contrast, when O_2 flow rate increases, the halogenated silicon etch products have a greater probability to be oxidized when they reach the chamber wall surfaces (i.e., their effective sticking probability increases with O_2), leading to a larger deposition rate of the SiO_X layer on the walls: even if the etch rate increases at low O_2 gas flow, the concentration of etch product in the gas phase decreases because they are lost at higher rates on the chamber walls, thanks to the oxidation reactions. The deposition rate of the silicon oxychloride film is proportional to both atomic oxygen flux and etch product flux. Therefore, as shown in Fig. 10 when the O_2 gas flow increases, the O flux increases but the flux of $SiCl_X$ product decreases, probably resulting in maxima in the deposition rate, as observed by Ullal *et al.*[44]

Finally, since Br reactivity towards oxide layers is low[45] (etch rate of SiO_2 in HBr-based plasmas is very low), Br loading is strongly reduced when the O_2 concentration in the gas phase increases. Furthermore, we have shown in previous studies that during the overetch step of a gate etch process, O atoms from the gas phase can easily substitute for Br atoms in the passivation layer formed on the silicon gate sidewalls.[40] Assuming that the same mechanism holds on the chamber walls, an increase in the O_2 concentration may generate a substitution of bromine by O in the film, which acts as a bromine source:

$$(SiO_ZCl_XBr_Y)_s+(O)_g\rightarrow(SiO_{Z+1}Cl_XBr_{Y-1})_s+(Br)_g. \tag{6}$$

This surface production mechanism of Br atoms is expected to be important since the reactor walls represent a very large area (approximately 15 times the wafer area).

In summary, when the O_2 concentration in the gas phase increases, silicon etch products reaching the chamber walls are oxidized and form a SiO_ZX_Y film (where X is an halogen atom), which covers the chamber walls. At the same time, the density of the film is increased by substitution of bromine by oxygen. This mechanism implies that the consumption (i.e., loading) of silicon-based etch products by the chamber walls increases with the O_2 concentration in the gas phase while the consumption of halogens such as Br and Cl decreases, in good agreement with the experimental results observed in Fig. 10.

An alternative explanation to the increase in Br and Cl densities with the O_2 flow could also be that the recombination rate of halogen atoms [Eq. (5)] changes with the O_2 gas flow. This phenomenon was shown[46] to be important when going from a clean chamber (Al_2O_3) to a seasoned chamber (SiO_X). The Cl and Br concentrations are 60% lower in the clean chamber than in the seasoned chamber (in good agreement with the measured surface recombination probability of Cl and Br atoms[47]). However, under our conditions, the largest part of the reactor wall surface is covered by a SiO_X layer (resulting from previous wafer processing) and the halogen

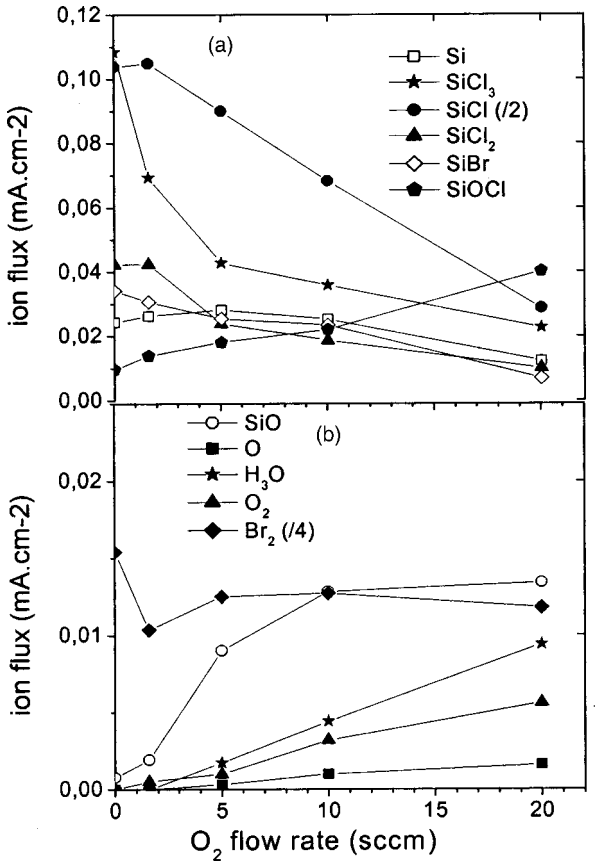

FIG. 11. Effect of the O_2 gas flow rate on the density of several ionized etch products (a) and on several oxygen containing ions (b). Conditions identical to Fig. 10.

atom recombination rate should be independent of the O_2 gas flow. Figure 11 shows that the Br_2^+ density is roughly constant for O_2 gas flows above 1.2 sccm, suggesting indeed that the halogen atom recombination rate is independent of the O_2 gas flow.

Finally, Fig. 11(a) shows that the O_2 flow rate modifies the etch product densities by the conjunction of two phenomena: first, the surface loss coefficient of these species increases with O_2, as explained previously, but the value of the sticking coefficient on the reactor walls is species dependent, and so is the loading effect. Second, the presence of atomic oxygen modifies the etch product distribution chemically sputtered from the wafer. As a result, the $SiCl_3^+$ density, which is large without O_2, drops dramatically as soon as O_2 is present in the mixture, while the $SiCl^+$ density is almost constant at low O_2 flow and then decreases almost linearly with it. At the same time the SiBr density decrease linearly with O_2 while the Si density passes through a maximum at 5 sccm of O_2. Finally, when O_2 is added to the gas mixture, some new etch products are formed during the etch process. Figures 11(a) and 11(b) show that although the $SiCl_XBr_Y$ densities drop with O_2 addition, two new ions originating from the etch product ionization increase in density with the O_2 flow, namely, SiO and SiOCl. At low O_2 gas flow, new products (SiO_XCl_Y) may contribute to the enhancement of the etch rate. Simultaneously, the halogen atom concentration increases, which should also enhance the etch rate. Finally, the measured (net) etch rate is the result of a competition between the silicon etching rate and the redeposition rate of the etch products (and ions) on the wafer. Since the density of the $SiCl_X$ species decreases with O_2 gas flow, so does their redeposition rate on the wafer. This decrease of the redeposition rate also results in an increase of the net etch rate with O_2 gas flow. However, it is difficult to estimate the contribution of these three mechanisms to the enhancement of the etch rate. Finally, it should be underlined that the density of O^+ and O_2^+ ions is very low even at large O_2 flow rates, suggesting that the substrate and reactor walls are also heavily loading O atoms in the system (producing $SiOCl_XBr_Y$ etch products from the wafer, and forming SiO_X layers by oxidation of the etch product at the chamber walls).

4. Influence of CF_4 addition

A recent trend in silicon gate patterning for complementary metal–oxide–semiconductor (CMOS) applications is to add CF_4 gas into the standard $HBr/Cl_2/O_2$ gas mixture to minimize the difference in etch rate between n^+- and p^+-doped polysilicon layers in dual gate etching, and simultaneously decrease the SiO_X layer deposition rate on the reactor walls. A recent study[48] has shown that when the CF_4 gas flow increases, the chemical composition of the layer coating the reactor walls changes from SiO_X to CF_X, going through a "clean" regime (when the gas flow ratio CF_4/O_2 is around 4), in which the reactor walls are basically kept clean.

The impact of 25 sccm CF_4 addition in the $HBr/Cl_2/O_2$ gas mixture previously studied (Fig. 3 and Table I) is summarized in Table II, illustrating the profound difference in the chemical nature of the ion flux between these chemistries. Table II shows that the sum of halogenated silicon ionized species is reduced to less than 25% of the total ion flux when 13% of CF_4 is added to the gas mixture, while Cl- and Br-containing ions now represent 53% of this flux. Furthermore, all the $SiCl_XBr_Y$ densities measured previously without CF_4 (see Table I) decrease in favor of SiF_X ionized etch products, while Br_2 and BrCl densities increase by a factor of more than 2. Besides, CF_X ions, and in particular CF_3^+, are detected in significant densities (CF_2^+ appears to be negligibly small).

TABLE II. Chemical composition of the ion flux bombarding the reactor walls in the 4 mTorr, HBr (110 sccm)/Cl_2 (70 sccm)/O_2 (5 sccm)/CF_4 (25 sccm) gas mixture, with 450 W rf source power and 100 W rf bias power. The numbers include the sum over all the isotopes of Cl and Br.

Species	Br	Br_2	BrCl	CF_3	SiF	SiCl	HBr	H_XCl	CF	$SiCl_3$	SiBr	SiF_3
% of total ion flux	15.9	13.5	12.5	9.2	9	7.3	7.1	4.3	2.9	2.6	2	1.2

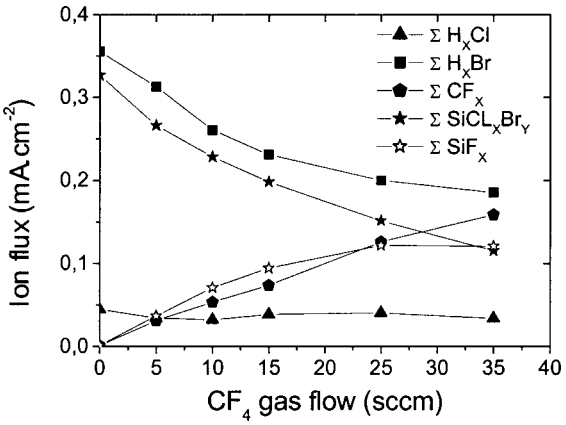

FIG. 12. Effect of the CF_4 gas flow on the density of halogenated silicon ions (sum of all of the $SiCl_XBr_Y$ with $0<X,Y<3$, and sum of all of the $SiBr_XCl_YF_Z$ with $0<X,Y,Z<3$), halogenated ions (sum of all H_XBr^{79-81} and H_XCl^{35-37} ions with $X=0-2$) and fluorocarbon ions (sum of CF^+, CF_3^+, and CHF_2^+). Process conditions are 4 mTorr total pressure in an HBr (110 sccm)/Cl_2 (70 sccm)/O_2 (5 sccm)/CF_4 (X sccm) gas mixture with 450 W rf source power and 100 W rf bias power.

The influence of the CF_4 gas flow on the ion flux chemical composition is shown in Fig. 12. We have separated the contributions of the halogenated silicon ionized etch product in two parts. One in which the halogen atoms are Cl and Br, and another consisting of silicon ions containing F atoms. As discussed above, CF_4 addition decreases the silicon bromine and chlorine etch products while fluorine-based silicon etch products (mostly SiF^+) are formed. This phenomenon may largely impact the SiO_X layer deposition rate on the reactor walls (and gates sidewalls), which are formed by $SiCl_XBr_Y$ oxidation on the surfaces. Etching of silicon by F atoms and CF_X radicals is also known to be more chemical than etching by Cl and Br atoms: the SiF_X etch products, which are more volatile than $SiCl_XBr_Y$, should be less reactive towards surfaces and more easily pumped away from the plasma chamber. Furthermore, the densities of CF_X^+ ions increases linearly with the CF_4 gas flow, and these ions can also participate in the removal of the SiO_X layers on the chamber walls. Therefore, the transition from the SiO_X to CF_X deposition regime on the chamber walls (and passivation layers[49] on the feature sidewalls) that have been observed[48] when increasing the CF_4 gas flow in such mixtures is well illustrated by the corresponding changes in densities of $SiCl_XBr_Y$ and CF_X precursor species in the gas phase.

The strong decrease of the Br^+ ion density (ΣHBr) with the CF_4 gas flow observed in Fig. 12 can be attributed to a large change in the surface recombination probability [Eq. (5)] of Br species when the composition of the layer deposited on the chamber walls changes from SiO_X to CF_X. This phenomenon will be discussed in a forthcoming article. The direct impact on Br (and Br_2) concentration in the gas phase with fluorocarbon addition in the gas phase is indeed obvious when comparing Tables I and II.

Finally, we observe one more time that the Cl^+ ion density is very small, indicating that chlorine-based species are loaded by the whole surfaces exposed to the plasma. This large loading of Cl atoms is indeed supported by XPS (Ref. 49) and multiple total internal reflection–Fourier transform infrared spectroscopy (MTIR–FTIR) (Ref. 50) measurements, which show very large concentrations of the chlorine element in the passivation and reactive layers present on the surfaces exposed to the plasma.

5. Impact on etching mechanisms

The presence of large amounts of silicon-containing ions in the ion flux bombarding the wafer has several consequences on etch rate and feature profile evolution. In particular, etch rates shall be reduced[31] when compared to the discharge condition where the ions consist solely of Cl^+ and Br^+. Indeed, we expect that the large amounts of $SiCl^+$ ions impacting the silicon surfaces will influence the chemical composition of the thin reactive layers driving the etching at the silicon surface. For a total gas flow of 100 sccm (Cl_2), the model from Lee, Graves, and Lieberman[31] predicts that the redeposition of the etch product (neutral and ions) on the surfaces exposed to the plasma is largely dominated by ionic redeposition underlying the importance of silicon-containing ions in the etching mechanisms. The reason is that the ions, which strike the walls with a typical energy of 30 eV, have a surface sticking probability independent of the surface halogen coverage while the neutrals will only stick on free-adsorption sites. It has also been suggested by Charles and Boswell[51] that silicon ions may also play a significant role in the deposition rate of the SiO_2-like layer on the reactor walls during SiO_2 plasma-enhanced chemical vapor deposition (PECVD).

Molecular dynamics (MD) simulation of energetic SiF_X ($X=0-3$) impact on silicon by Helmer and Graves[52] have also shown that direct reaction of these reactive ions with the surface takes place and is an important mechanism of the plasma surface interaction.

Apart from depositing on the surfaces exposed to the plasma, silicon-containing ions will also impact several peculiarities of the etched profiles such as sidewall tapering and microtrenching. As an example, when the silicon area being etched increases or the bias power increases, the ions bombarding the wafer are "less reactive" (since the $SiCl_X^+/Cl^+$ ratio increases): the difference in reactivity may deeply influence the profile distortion. Microtrenching is attributed to a focalization of the ion bombardment at the edges of the structures being etched after reflection of the ions at grazing angles on the mask and feature sidewalls. It has been suggested[9,11] and observed experimentally[32] that, depending on the nature of the ions (i.e., Br^+ or Cl^+), reflection on the feature sidewalls can be more or less specular, explaining the difference in the microtrenching amplitude between chlorine and bromine. Our result suggest that the real case is even more complicated since depending on the initial chemistry, between 20% and 50% of the ions reflected on the sidewalls are $SiCl_XBr_Y$ (often with $x,y\leqslant 1$). These ions are much less reactive than Cl^+ or Br^+ and their presence will minimize the microtrenching amplitude. Modelization, and in particular molecular dynamic simulations, will be required to evalu-

ate the exact impact of the $SiCl_XBr_Y^+$ ion bombardment on the profile simulation.

The etch selectivity between mask and silicon and between silicon and the SiO_2 gate dielectric, in a gate etch process, may also be impacted by the presence of high densities of silicon-containing ions. We expect both selectivities to decrease with an increase in the silicon ion concentrations in the gas phase. As an example, it is well known that the etch selectivity to the gate oxide decreases when the silicon area to be etched on the wafer increases: this is very simply related to an increase in silicon ion densities in the gas phase, which render the etch more physical than chemical.

Other phenomena are potentially impacted by the presence of heavy silicon-containing ions in the gas phase of high-density plasmas used for gate etching. Differential charging effects, which come from the difference in directionality between ions and electrons in high aspect ratio structures, should be also largely impacted by the presence of light ions such as H^+ and heavy ions such as $SiCl_XBr_Y^+$ (since ion deflection towards the gate sidewall is influenced by the ion mass and the ion energy distribution function). Low mass ions such as H^+ (which are abundant in HBr-based discharges) present a bimodal distribution function in energy due to the time modulation of the rf bias voltage. The low energy ions of the bimodal distribution function will be more easily deflected by the negative charge generated on top of the insulating mask while the high energy H^+ protons will be much less affected. On the other hand, we are expecting a single peaked ion energy distribution function for heavy ions such as $SiCl_XBr_Y^+$. In principle, they should be less easily deflected by the electric field induced in high aspect ratio structures since (1) they get accelerated by the full sheath potential and (2) the electrostatic force driving the deflection is inversely proportional to the ion mass. Consequently, modelization of the electrical phenomena occurring in these structures must take into account the large silicon-based ion densities reaching the wafer surface to have a good enough predictive capability.

IV. CONCLUSION

We have investigated the identity of the ions bombarding the walls of an industrial ICP operated in $HBr/Cl_2/O_2$ with or without CF_4 used for silicon gate etching. Calibrated mass spectrometry indicates that the ion flux composition greatly differs from widespread ideas since up to 50% of the ions bombarding the reactor walls are ionized silicon etch products. Furthermore, we demonstrate that O_2 and CF_4 addition to halogen gases deeply modifies the loading of halogens and silicon etch products on the reactor wall and wafer surfaces. The addition of CF_4 also leads to a deep modification of silicon-based ions bombarding the wafer.

[1]M. A. Lieberman and A. J. Lichtenberg, *Principle of Plasma Discharges and Material Processing* (Wiley, New York, 1994).
[2]V. Vahedi, D. Cooperberg, J. M. Cook, and R. A. Gottscho, Proceedings of the 20th Symposium on Dry Process, Tokyo (1998).
[3]V. Vahedi, J. Daugherty, S. Huang, D. Cooperberg, and R. A. Gottscho, Proceedings of the 21th Symposium on Dry Process, Tokyo (1999).
[4]J. P. Chang, A. P. Mahorowala, and H. H. Sawin, J. Vac. Sci. Technol. A **16**, 217 (1998).
[5]M. A. Vyvoda, M. Li, and D. B. Graves, J. Vac. Sci. Technol. A **17**, 3293 (1999).
[6]S. Hamaguchi and M. Dalvie, J. Vac. Sci. Technol. A **12**, 2745 (1994).
[7]M. Tuda, K. Nishikawa, and K. Ono, J. Appl. Phys. **81**, 960 (1997).
[8]M. Tuda, K. Ono, and K. Nishikawa, J. Vac. Sci. Technol. B **14**, 3291 (1996).
[9]M. A. Vyvoda, M. Li, D. B. Graves, H. Lee, M. V. Malyshev, F. P. Klemens, J. T. C. Lee, and V. M. Donnelly, J. Vac. Sci. Technol. B **18**, 820 (2000).
[10]G. S. Hwang, C. M. Anderson, M. J. Gordon, T. A. Moore, T. K. Minton, and K. P. Giapis, Phys. Rev. Lett. **77**, 3049 (1996).
[11]S. Abdollahi-Alibeik, J. P. McVittie, K. C. Saraswat, V. Sukharev, P. Schoenborn, and V. Sukharev, J. Vac. Sci. Technol. A **17**, 2485 (1999).
[12]V. M. Donnelly, J. Vac. Sci. Technol. A **14**, 1076 (1996).
[13]V. M. Donnelly, J. Appl. Phys. **79**, 9353 (1996).
[14]M. V. Malyshev, V. M. Donnelly, A. Kornblit, and N. A. Ciampa, J. Appl. Phys. **84**, 137 (1998).
[15]M. V. Malyshev, N. C. M. Fuller, K. H. A. Bogart, V. M. Donnelly, and I. P. Herman, Appl. Phys. Lett. **74**, 1666 (1999).
[16]M. V. Malyshev and V. M. Donnelly, J. Appl. Phys. **87**, 1642 (2000).
[17]K. V. Guinn, C. C. Cheng, and V. M. Donnelly, J. Vac. Sci. Technol. B **13**, 214 (1995).
[18]F. H. Bell, O. Joubert, and L. Vallier, J. Vac. Sci. Technol. B **14**, 1796 (1996).
[19]M. E. Barone and D. B. Graves, J. Appl. Phys. **77**, 1263 (1995).
[20]J. P. Chang and H. H. Sawin, J. Vac. Sci. Technol. A **15**, 610 (1997).
[21]H. F. Winter and J. W. Coburn, Surf. Sci. Rep. **14**, 161 (1992).
[22]M. W. Kiehlbauch and D. B. Graves, Proceedings of the 23th Symposium on Dry Process, Tokyo (2001).
[23]N. S. J. Braithwaite, J. P. Booth, and G. Cunge, Plasma Sources Sci. Technol. **5**, 677 (1996).
[24]H. Singh, J. W. Coburn, and D. B. Graves, J. Vac. Sci. Technol. A **18**, 299 (2000).
[25]H. Singh, J. W. Coburn, and D. B. Graves, J. Vac. Sci. Technol. A **17**, 2447 (2000).
[26]R. Foest, J. K. Olthoff, R. J. Van Brunt, E. C. Benck, and J. R. Roberts, Phys. Rev. E **54**, 1876 (1996).
[27]Y. W. Wang and J. K. Olthoff, J. Appl. Phys. **85**, 6358 (1999).
[28]A. N. Goyette, Y. W. Wang, M. Misakian, and J. K. Olthoff, J. Vac. Sci. Technol. A **18**, 2785 (2000).
[29]Y. W. Wang, M. Misakian, A. N. Goyette, and J. K. Olthoff, J. Appl. Phys. **88**, 5612 (2000).
[30]F. Neuilly, Ph.D. thesis, Université Joseph Fourier, France (2000).
[31]C. Lee, D. B. Graves, and M. A. Lieberman, Plasma Chem. Plasma Process. **16**, 99 (1996).
[32]S. A. Vitale, H. Chae, and H. H. Sawin, J. Vac. Sci. Technol. A **19**, 2197 (2001).
[33]C. Lee and M. A. Lieberman, J. Vac. Sci. Technol. A **13**, 368 (1995).
[34]M. E. Weber and P. B. Armentrout, J. Phys. Chem. **93**, 1596 (1989).
[35]D. J. Oostra, A. Haring, R. P. van Ingen, A. E. de Vries, and G. N. A. van Veen, J. Appl. Phys. **64**, 315 (1988).
[36]F. H. M. Sanders, A. W. Kolfschoten, J. Dieleman, R. A. Haring, A. Haring, and A. E. de Vries, J. Vac. Sci. Technol. A **2**, 487 (1984).
[37]R. S. Goodman, N. Materer, and R. Leone, J. Vac. Sci. Technol. A **17**, 3340 (1999).
[38]N. Materer, R. S. Goodman, and R. Leone, J. Vac. Sci. Technol. B **18**, 191 (2000).
[39]G. S. Oehrlein, J. F. Rembetski, and E. H. Payne, J. Vac. Sci. Technol. B **8**, 1199 (1990).
[40]L. Desvoivres, O. Joubert, and L. Vallier, J. Vac. Sci. Technol. B **19**, 420 (2001).
[41]K. Nojiri, K. Tsunokumi, and K. Yamazaki, J. Vac. Sci. Technol. B **14**, 1791 (1996).
[42]N. Ozawa, T. Matsui, and J. Kanamori, Jpn. J. Appl. Phys., Part 1 **34**, 6815 (1995).
[43]G. C. H. Zau and H. H. Sawin, J. Electrochem. Soc. **139**, 250 (1992).
[44]S. J. Ullal, H. Singh, V. Vahedi, and E. S. Aydil, J. Vac. Sci. Technol. A **20**, 499 (2002).
[45]M. Nakamura, K. Lizuka, and H. Tyano, Jpn. J. Appl. Phys., Part 1 **28**, 2142 (1989).

[46]S. Xu, Z. Sun, X. Qian, J. Holland, and D. Podlesnik, J. Vac. Sci. Technol. B **19**, 166 (2000).
[47]G. P. Kota, J. W. Coburn, and D. B. Graves, J. Vac. Sci. Technol. A **17**, 282 (1999).
[48]S. Xu, Z. Sun, A. Chen, X. Qian, and D. Podlesnik, J. Vac. Sci. Technol. A **19**, 871 (2001).
[49]G. Cunge, L. Vallier, O. Joubert, J. Foucher, and X. Detter, Proceedings of the 49th AVS, San Francisco, CA (2001).
[50]A. R. Godfrey, S. J. Ullal, L. B. Braly, E. A. Edelberg, V. Vahedi, and E. S. Aydil, Rev. Sci. Instrum. **72**, 3260 (2001).
[51]C. Charles and R. W. Boswell, J. Appl. Phys. **81**, 43 (1997).
[52]B. A. Helmer and D. B. Graves, J. Vac. Sci. Technol. A **15**, 2252 (1997).